Comparative of different Direct Drive architectures

Pablo F. Miaja
Power supply systems group
University of Oviedo
Gijón, Spain
fernandezmiapablo@uniovi.es

Andreas Franke
Electrical Power Management section (TEC-EPM)
European Space Agency
Noordwijk, The Netherlands

Denis Estublier
Electric Propulsion section (TEC-MPE)
European Space Agency
Noordwijk, The Netherlands

Christian Brandt
Electrical Power Generators section (TEC-EPG)
European Space Agency
Noordwijk, The Netherlands

Gustavo Alvarez
Electrical Power Management section (TEC-EPM)
European Space Agency
Noordwijk, The Netherlands

Manuel Arias
Power supply systems group
University of Oviedo
Gijón, Spain

I. Abstract:

The increase in usage of electrical propulsion systems in spacecraft has raised the research in methodologies that seek to increase the energy and mass efficiency of such systems. Looking at how Hall Effect thrusters are powered several Direct Drive architectures have been proposed. This papercompares several of them to assess which one would have the better performance.

II. Introduction:

The objective of the paper is to assess different Direct Drive (DD) power topologies aimed towards supplying Hall Effect Thrusters (HET) in Electrical Propulsion (EP). Nowadays, HETs are supplied from the power bus through a Power Processing Unit (PPU).

A typical PPU schematic is represented in Figure 1a. The PPU is in charge of controlling the HET to achieve the desired thrust. It controls the gas flow both for the thruster and the hollow cathode interacting with the gas supply system. It provides the current. to the magnet via the Magnet Supply to achieve the desired magnetic field in the HET. It prepares the plasma ignition through the heater, provided by the Heater supply, and powers the electron generation in the hollow cathode though the Keeper Supply. Finally, it provides the anode with the voltage and current necessary to generate the discharge between Anode and Cathode, which in turn generate the thrust. The power consumed in this discharge is supplied through the Discharge supply.

The physics of the discharge between Anode and Cathode is very complex [1], [2]. This discharge will have an IV curve that above a certain voltage, usually in the hundreds of volts being 300 V a common voltage, behaves like a current source, demanding a DC value proportional to the gas flow. In addition, several oscillations will appear. The most important have frequencies mostly in the tens of Kilohertz range and have an amplitude up to 100% of the DC value. The mission of the Filter Unit is to avoid these oscillations to propagate into the discharge supply. Therefore, the Discharge supply will see the discharge between anode and cathode almost as a pure DC current source.

In order to guarantee the discharge between anode and cathode and prevent a discharge between the anode and the structure the discharge supply output will be referenced to the Cathode Reference Point (CRP) instead of the spacecraft (SC) ground, therefore the discharge supply typically is a galvanically isolated one. However, there are some approaches [3] that include an additional supply, called the CRP Supply that sense the current through the anode and its return, the current through the cathode, and bias the CRP so the difference is zero. This approach is represented in Figure 1b. The CRP source must process all the supply current but at a lower voltage and hence at a lower power.

Inside the PPU, the discharge supply is the element that processes most of the power. HETs range from hundreds of watts to few kW, being 5 kW a reasonable number, and therefore its efficiency is critical towards the SC design. The high power processed impacts the thermal design of the PPU and the total SC. Moreover, the discharge power is converted from the Solar Array (SA) or the battery, first by the Power Conversion and Distribution Unit (PCDU) and then by the Discharge Power supply. Thus there are two cascaded power conversions, with the associated efficiency penalty. Then the power demand of the discharge supply affects the PCDU design and the whole SC design. Therefore, DD topologies have been proposed to supply the discharge power demand directly from a dedicated SA [4], [5], so there are no power conversions between the SA and the discharge, thus avoiding the design of the Discharge Supply and preventing this power by being processed first by the PCDU. One of the main disadvantages of this system is that the SA that must supply the EP has to provide voltages above 300 V, which is a technological challenge in the space environment [6], [7]. Moreover, the power generated by these EP dedicated SA (EP-SA) cannot be utilized by the rest of the SC systems when

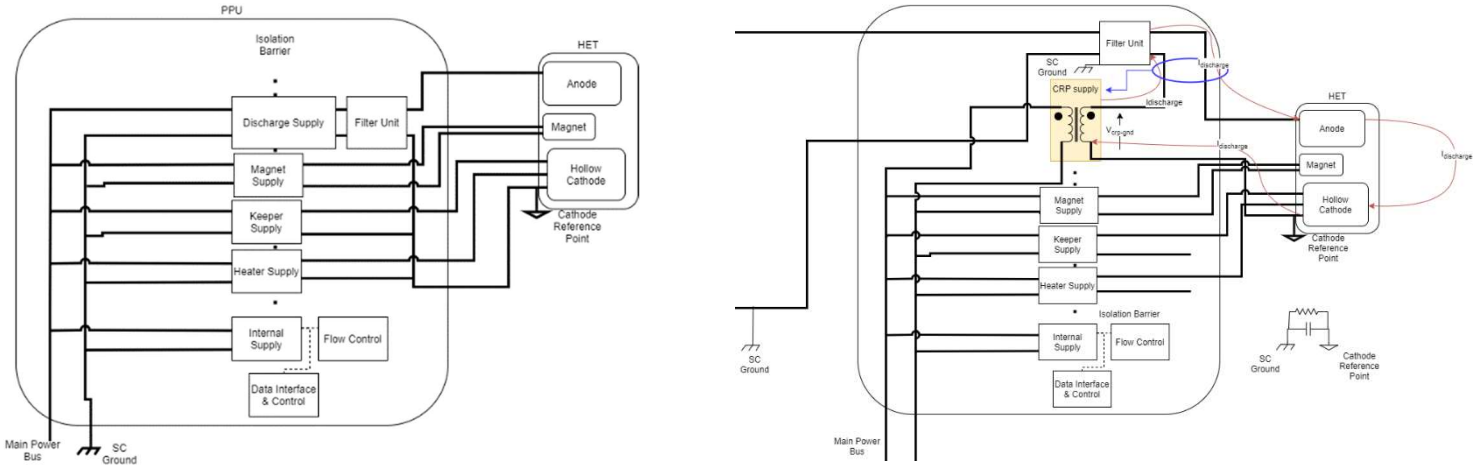

(a) (b)

Figure 1: PPU alternatives: a) Isolated b) CRP supply

EP is not in use. In many cases, the amount of time that the EP is on during a mission is rather low, thus it would be important to utilize the installed SA power for other uses rather than just for the discharge supply while the EP is on.

In this work several DD alternatives have been investigated. The goal is to provide an evaluation of which alternative would be the best to fulfil different SC power demand, especially regarding the optimization of SA surface. All the alternatives will allow to utilize the SA dedicated to the Discharge Supply to supply the power bus when the EP is not in use. Also, all of them aim to simplify the discharge supply and introduce minimal new developments so could be implemented without new significant developments in the domains of SA design and power conversion techniques.. Models regarding efficiency, mass and dissipation for the different constituent parts were developed in Python to compare all the architectures.

This work is organized as follows. Section III describe the different power architectures which have been studied in this work. Section III.C addresses the S3R based ones and section III.D the ones based in DC/DC converters with MPPT capabilities. The traditional architecture, with two cascaded power conversions, and a derivation of it is addressed in section III.E. Section IV establishes the comparison among them. Section IV presents the methodology and the results Python tool that calculate the figures used to make the comparison. Finally, the main conclusions of the study are addressed in section V.

III. ARCHITECTURES OF THE STUDY:

A. Assumptions:

The study covers the two main power systems used by European SC. Power systems using direct energy transfer based on the Sequential Switching Shunt Regulator (S3R) and based on DC/DC converters with Maximum Power Point Tracking (MPPT) capabilities. Both include modifications to deal withs DD systems.

The following assumptions have been made:

- The power bus voltage is fixed. The results can then be applied for the regulated bus or for an unregulated bus once the battery is fully charged [8] which is often the case for turning on the EP. In the tool the bus voltage can be manually set. Given the power demanded by EP it will be typically 100 V.
- Auxiliary supplies relevant for the study such as the CRP supply have been modelled in terms of efficiency and power density after a commercial isolated DC/DC converter [9].with a 100% margin for the power density. Therefore, the efficiency is 90% regardless of the power processed and the power density considered for this supply is 0.008 Kg/W and. The power density multiplied by the power processed gives the mass used in the study for the analysed case. The output voltage of a CRP supply is assumed to be 5 V [3]. The current processed is the discharge current. This current would be 16 A for 5 kW HET operating at 300 V. Hence the CRP supply must deliver 83 W. Mass wise it would seem to be a gross overestimation but given the low power it does not penalize excessively the mass comparison. Moreover, as the reference model processes a similar power it may be more accurate than it could seem at first sight.
- The DC/DC converters interfacing the SA is based on the one described in [10]. Its efficiency is assumed to be 95%, regardless of the power processed and the power density is 0.0016 Kg/W.
- The S3R power system is based on the one presented in [11]. The efficiency is 98.5% regardless of the power processed and the power density is assumed to be 0.00084 Kg/W.
- The PPU design regarding gas flow control, heaters, magnets, etc. is assumed to be the same regardless the DD option. The different options will affect the mass of the system by replacing the discharge supply. For comparison purposes it will be assumed that a typical discharge supply is 0.0018 kg/W and 90% efficiency.
- Some of the options make use of the results of the previous ESA funded activity [12]. In this work an unregulated isolated DC/DC converter, DCX in this work, is presented. These DCX are modular so several DCX blocks can be arranged to have an optimized design. For the present study designs using these DCX have been evaluated for different DD options. The efficiency per module is calculated from theoretical values using space grade components. For the mass of a module, it is assumed to be the one of the magnetic transformers needed by the design multiplied by two.

- Solar Cells are assumed to be 3G30 from AzurSpace [13]. No radiation degradation has been considered. The SA is assumed to work in the conditions that the Solar Cells have been measured. Then the short-circuit current is 0.475 A, open circuit voltage is 2.7 V, maximum power point voltage is 2.457 V and maximum power point current is 0.4428 V. The surface is 30.18 cm^2. This is a depart from traditional sizing methods in which the SAs are sized at endo of life. However, given the different nature of the missions and the different degradations faced, it was deemed that a fairer comparison could be made with SAs at beginning of life.
- The mass of the SA has been extracted using the figures from Airbus Sparkwing modular solar panels from Airbus DS. The 50 V model has panels of 4.47 m^2 in which 312 cells can be fitted. Each of these panels have a weight of 3.8 kg. Once the tool calculates the number of cells needed to cover the power demand the SA mass is calculated by computing the number of panels needed and then multiplying it by the mass of the panel.

B. Overview of the topologies:

An overview of the different topologies under study is performed in this section. Here, block schematics of the different architectures are depicted. Figure 2 shows the traditional architecture plus one based on it in which the discharge supply of the PPU is replaced by an unregulated DCDC converter, a DCX. Topologies based on S3R are depicted in Figure 3. Finally, the ones based on solar array regulators based on DC/DC converters with MPPT capabilities are shown in Figure 4. In all these figures, the power flow is represented by arrows. Low voltage SAs, with MPP close to 100 V are depicted in blue. Green blocks represent SA with MPP close to the operating voltage of the HET, around 300 V. Solar Array Regulators, either S3R based or DC/DC with MPPT based are represented in yellow. These stages take an input unregulated voltage and deliver it at the output tightly regulated. Unregulated voltage transformations stages, DCX, are represented in red. As aforementioned DCX provide at its output a scaled version of the voltage at its input. The bus, represented in purple, performs the distribution of electrical power to the loads which consume the electrical power. The loads are represented in grey.

The traditional system in which a PPU Discharge supply provides the HET with a regulated voltage extracting power from the bus is shown in Figure 2a. This model is introduced for comparison purposes. A variation of this, in which the discharge supply is replaced by a DCX that provides a scaled version of the bus is shown in Figure 2b.

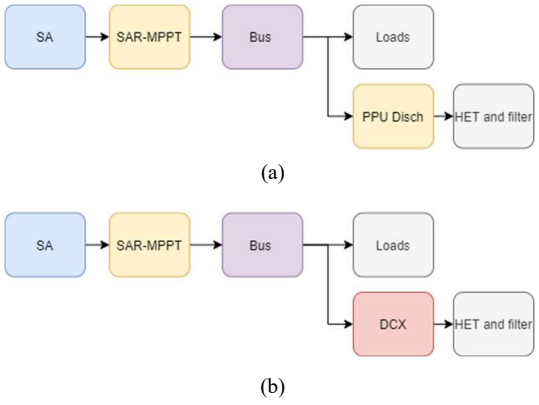

Figure 2: Traditional topologies: (a) Traditional PPU design, (b) DCX discharge supply

The S3R based systems are depicted in Figure 3. The Pure DD system, which has a HV SA to power the HET is depicted in Figure 3a. This HV SA system can be either connected to the HET or to the input of an S3R regulator to provide power to the bus. Isolated DD system can be seen in Figure 3b. No HV SA is needed in this case. The HET is supplied through a DCX that scale the SA voltage to HET demands. When HET is not in use the SA sections are used by the DCX to supply the HET. This is also the case of the Semi-Isolated system depicted in Figure 3c. In this case one of the sections is directly connected to the HET. The output voltage of this section is combined with the output of DCX to properly supply the HET.

The systems based on MPPTs are depicted in Figure 4. In the Single LV SA depicted in Figure 4a a low voltage SA is scaled up to supply a HET, at the same time the remainder of the power is used to supply the bus. The same approach is used in the Separated LV SA systems shown in Figure 4b. In this case the SAR-MPPT has two independent inputs, and the EP SA is sized to supply the HET power demand. The SAR-MPPT will get all the remaining power from the EP-SA and the rest from the SA. The same concept is applied in Figure 4c and Figure 4d, where HV SA are used for the same purpose. These SA are scaled down to supply the bus through the SAR. Finally, once high voltage SARs are developed, high voltage SA can supply both the bus and the HET as seen in Figure 4e and Figure 4f. Even inf the blocks are labelled as SA they can be thought as sections on the same SA physical structure.

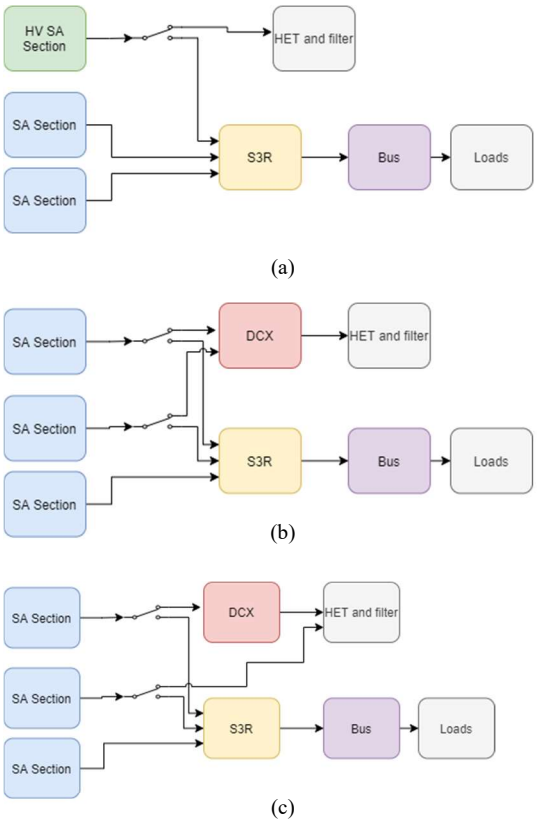

Figure 3: S3R based topologies: (a) Pure DD, (b) Isolated, (c) Semi-isolated.

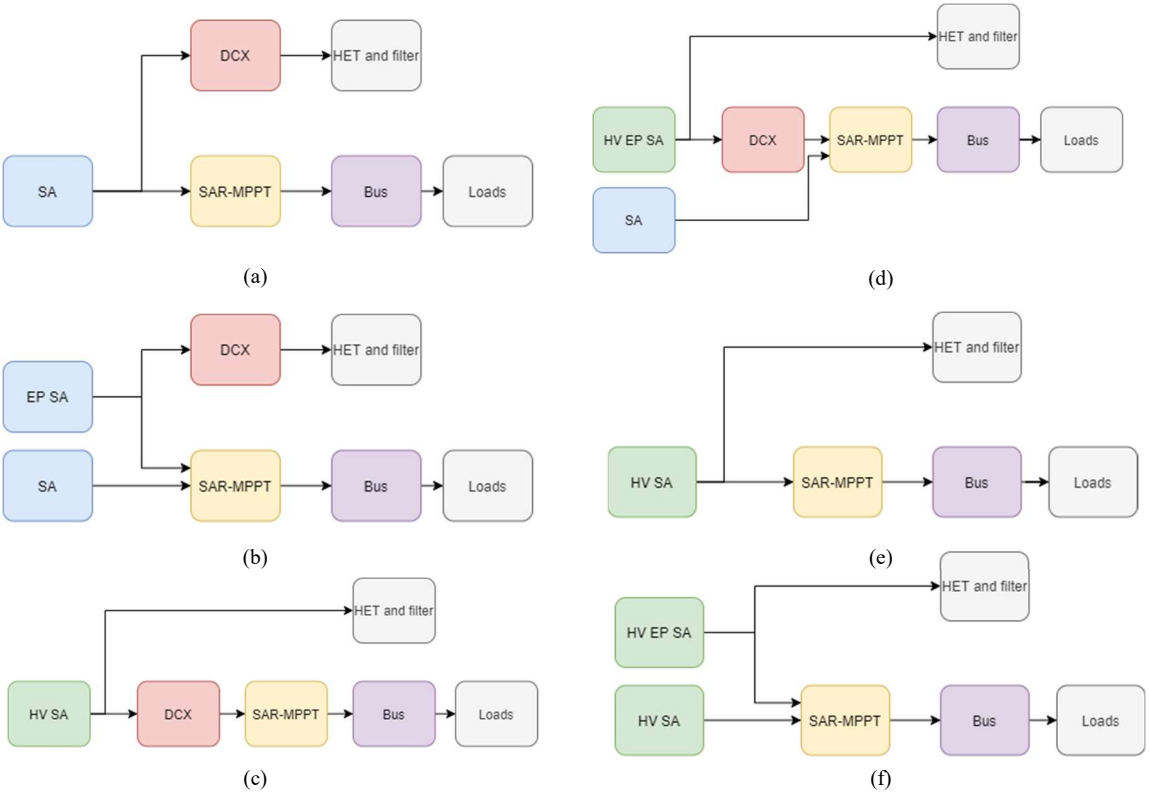

Figure 4: MPPT based topologies: (a) Single LV SA, (b) Separated LV SA, (c) Single HV SA, (d) Separated HV SA, (e) Single HV system, (f) Separated HV system.

C. S3R based topologies:

In the S3R power system several solar sections are directly connected to the power bus through a diode. These SA sections are sized so at the bus voltage the SA behaves as a current source injecting current to the bus. In case that the current injected is higher than the demand, the bus voltage would rise. To prevent that, a SA section is shunted, so less current is injected in the bus.

In the traditional Direct Drive approach, a SA would be connected directly to a HET. As aforementioned the HET through the filter unit would behave as a DC current source [1], [2]. Then, to avoid connecting two current sources in series, which will be unstable, the SA has to be sized so the HET current demand lies in the region that makes the SA behave as a current source. This is illustrated in Figure 5(a) where a SA IV curve has been represented. Two points, indicated by red stars are displayed, the leftmost one is in the current source region and the rightmost in the voltage source one. If the HET DC current demand intersects the SA IV at the rightmost star, small variations in the HET current will imply small changes in the SA voltage. Thus, this is a stable point. If the SA and the HET current demand intersect near the leftmost star, small HET current variation will imply big SA voltage variations, rendering this point unstable.

Several power architectures using the S3R approach have been assessed.

1) Pure Direct Drive:

a) Architecture description:

The Pure Direct Drive approach, depicted in Figure 3a., relies on having a High Voltage SA (HV SA) that will power the HET The SA should be designed so its maximum power point is located at a voltage higher but close to the HET operation and its current is also higher but close to the maximum discharge current. Therefore, the discharge current will determine a voltage over the HET situated in the voltage source region of the SA, including adequate margins for failure or degradation. In this scheme the discharge between anode and cathode is guaranteed by a CRP supply.

The voltage over the HET depends on the current extracted from the SA, which is the discharge current. This discharge current is proportional to the gas injected in the HET and the PPU can control it via the gas flow control. The lower the current the higher the voltage. This may have an impact on the HET as specific impulse is proportional to the HET voltage and the thrust is proportional to the gas flow [2].

To utilize the HV SA for providing power to the bus when the EP is not in use a switch connects the positive of the HV SA to an S3R section input. This switch could be implemented via relays or MOSFETs. When the EP is in use the PPU turns the switch off and the power only flows to the HET. If the HET is off the PPU turns the switch on and the power could be extracted using the S3R system. Depending on the Main Error Amplifier Voltage the S3R will shunt the HV SA or connect it to the bus. If the HV SA is connected to the bus the voltage across it will be the bus voltage, which will be much smaller than the maximum power point of the HV SA. Then the HV SA will behave as a current source injecting current in the bus. This is illustrated in Figure 5(a), where the IV curve of a SA designed to provide a 300 V 5 kW HET is displayed. The current at 300 V is 17 A and at 100 V is 18 A. Figure 5(b) displays the power output of the same SA. It illustrates the main drawback of the pure DD approach. A HV SA designed to provide 5 kW to the HET can only deliver 1.8 kW to the bus. Therefore, when the EP is not in use most of the power provided by the SA cannot be used directly by the bus.

For this approach to be used SA capable of supplying voltages compatibles to HETs are needed. This means SA voltages in the 300 V range, which are currently under development.

2) Isolated Direct Drive:

a) Architecture description:

To avoid using a HV SA it could be possible to scale the voltage and current provided by a SA to the voltage requirements of the HET. This can be accomplished by using

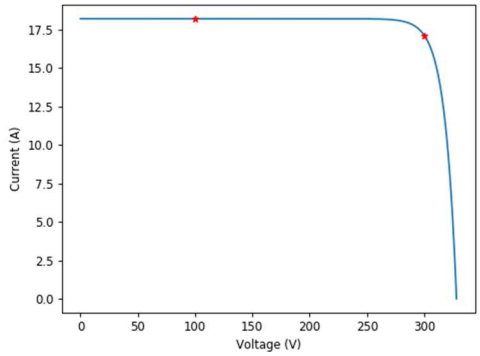

(a)

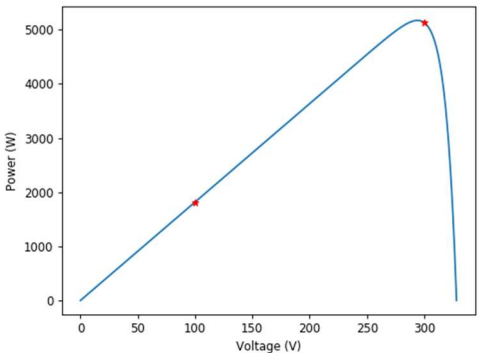

(b)

Figure 5: IV (a) and (b) power curves for a SA designed for a Pure DD

a DCX. These DCX are isolated so as an additional advantage there is no need to include the CRP supply in the design. However, this means that the full power demanded by the HET is processed by the DCX, which the consequent losses. Nevertheless, as the DCX efficiency is high the losses shall be much smaller than in the traditional scheme where the power is processed first by the PCDU and then by the Discharge Supply of the PPU.

The DCX will provide a scaled version of the SA IV. This is shown in Figure 6 where a DCX with an output to input ratio of 3 is shown. In it a SA with a maximum power point voltage V_{mp} of 100 V and maximum power point current, I_{mp}, of 6 A is scaled by the DCX so at the output of the DCX the SA will be seen as one with a V_{mp} of 300 V and a I_{mp} of roughly 2 A. Therefore, the HET will see that it is connected to a 300 V, 2 A maximum power point SA. As it can be seen the power delivered is almost the same, only the losses on the DCX need to be considered.

If a single SA section has enough power for the discharge of the HET the simplest approach is to connect the SA section through a DCX to the HET. The DCX will scale the SA section so the HET sees it as a HV SA as in the pure DD option, with the discharge current in the voltage source side of the virtual HV SA. Again, as in the pure DD option a switch allows the section to be connected to a S3R input. When the EP is not in use all the MOSFETs of the DCX will be turned off, disconnecting the HET from the SA and the switch is closed. When the EP is in use the switch is open and the DCX starts switching, presenting the HET with a scaled version of the SA section. In this case the SA section can be designed as it is usual in the S3R designs. The HET will see a Solar Array so the maximum power point is the section maximum power point voltage and current scaled by the DCX turns ratio, n_{DCX}. This is what it is indicated in Figure 3b.

If the HET demands more power than a single section can provide the scheme can be repeated with several sections, being $m_{sections}$ the number of SA sections devoted to HET

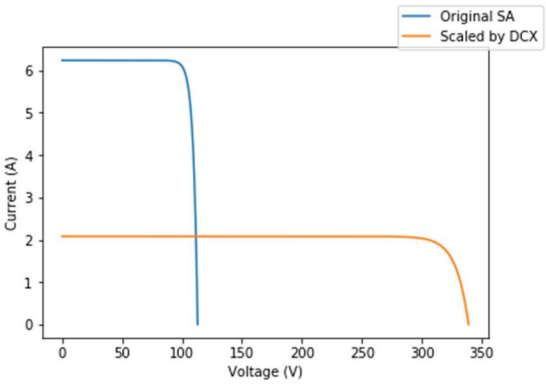

Figure 6: SA IV curve scaled through DCX

operation. It is assumed that all the sections are equal. For each of the sections to power the HET there will be an isolation switch and a DCX. When the EP is not in use the DCX are off and the switches are on, allowing these sections to be connected to the S3R. When the EP is on the switches are off and the DCX are turned on. Thus, all the sections connected through the DCX will behave as a single HV SA with a maximum power point voltage:

$$V_{mp} = n_{DCX} \cdot V_{mp\_section} \quad (1)$$

$$I_{mp} = m_{sections} \cdot {}^{I_{mp_{section}}}/_{n_{DCX}} \quad (2)$$

Construction wise the DCX enables a protection between the SA sections and the HET. As the DCX is based into full bridges if all the MOSFETs are commanded off the input is isolated from the output. Then, the disconnection of the DCX will isolate the Filter Unit and the anode of the HET from the SA.

3) Semi-Isolated Direct Drive:

a) Architecture description:

As a variation of the Isolated Direct Drive series option, the semi isolated one is presented here. The idea is to reach the desired voltage through the combination of several, $m_{sections}$, low voltage SA sections as in the Isolated Direct Drive series option. However, there is a section which is directly connected, without a DCX, to the return of the HET. The others are connected in series to this one through DCX. In this topology the CRP supply is needed to guarantee the discharge between anode and cathode. The block scheme of this architecture can be seen in Figure 3c.

The topology works as the Isolated Direct Drive. The discharge current, I_{dis}, will circulate through the non-isolated SA section and through the output of the DCX. This current will make the non-isolated SA section to present a voltage according to its IV curve. The SA must be sized so with I_{dis} the SA operates in its voltage source region.

$$V_{SA\_non\_iso} = f_{IV}(I_{dis}) \quad (3)$$

For the sections that are connected through DCX, I_{dis} will be transferred to the input of the DCX as I_{in} so

$$I_{in} = {}^{I_{dis}}/_{n_{DCX}} \quad (4)$$

And then assuming that all the sections are the same

$$V_{SA_{iso}} = f_{IV}(I_{in}) \quad (5)$$

This voltage will be transferred to the output of the DCX properly scaled

$$V_{DCX} = n_{DCX} \cdot V_{SA_{iso}} \quad (6)$$

The HET will then see a total voltage of

$$V_{HET} = (m_{sections} - 1) \cdot n_{DCX} \cdot V_{SA_{iso}} + V_{SA\_non\_iso} \quad (7)$$

If we design all the sections to be equal for S3R operation and under the HET operation all sections provide the same power, then the only solution will be to have a turn ratio n_{DCX}=1. Then, the HET will see a solar array with a maximum power point of

$$V_{mp} = m_{sections} \cdot V_{mp\_section} \quad (8)$$

$$I_{mp} = I_{mp\_section} \quad (9)$$

Which is the same as the isolated DD option in series if the DCX turn ratio is one. The advantage is that the power provided by the non-isolated section is directly supplied to the HET without being converted by the DCX. Then the efficiency in providing the HET will be bigger. However, the CRP supply is needed, which may hamper the global efficiency.

D. DC-DC converter-based SAR with Maximum Power Point Tracking Capabilities:

Whilst the S3R power system is very efficient it cannot track the Maximum Power Point of a SA. Although, some approaches have been made in this regard they require the S3R feeding a variable voltage bus[14], [15], which is not currently allowed for the main power bus of SC.

Maximum power tracking capabilities are well regarded when the SC must face varying illumination conditions such as in interplanetary missions facing many different distances to the Sun or in LEO missions facing many long eclipses.

In MPPT architectures all the SA sections are connected. The SA is designed to work in the voltage source region. It is important to note that the DC/DC converter will extract power from the SA by demanding a current at a voltage higher that V_{mpp}. In regulated bus architecture the MEA will dictate how much current the DC/DC converter needs to inject into the bus. Only if the power demand matches or exceeds the SA power generation will the DC/DC converter lock into the Maximum Power Point of the SA. In this situation the DC/DC converter does not regulate it output voltage nor the current. Its control will be targeted into keeping its input voltage and current locked into MPP.

There are many MPPT methods, an overview can be seen in [16]. For SC applications one of the most used is the incremental conductance method. In this method the input voltage and current of the DC/DC converter oscillates around the MPP [17], which translates into the output current. These oscillations appear in the hundreds of Hz range. Yet, these oscillations do not reflect on the bus voltage as they are damped by means of the BDR or the battery.

Several options have been considered, most of them make use of a DCX to feed the anode of the HET directly from the SA.

1) Single LV SA:

a) Architecture description:

The schematic of the proposal is displayed in Figure 7. The idea is that the SC has only on SA interfacing the Solar Array Regulator (SAR). The SA is sized accordingly to the power demand of the bus and the HET. Then the V_{mp} in nominal conditions will be close to the bus voltage. If the SAR uses a Buck or Buck like topology the V_{mp} will be slightly higher, around 10% more.

In parallel with the input of the SAR a DCX will directly power the HET. This DCX will scale the SA voltage to the operating voltage of the HET. The turns-ratio will translate the V_{mp} to the recommended operating voltage of the HET. The DCX will be sized for the power of the HET and in addition it will provide galvanic isolation guaranteeing the discharge between anode and cathode.

When the HET is on, the SAR will see less current available. Therefore, for the same power demand in the bus the MEA will react increasing its voltage asking for more current. Eventually locking in the MPP. This is represented in Figure 8.

It is important to note that the voltage at the HET will not be regulated. The HET will be seeing, scaled through the DCX, the voltage of the SA corresponding to the total current demand, the one imposed by the SAR to cover the bus demand and the one at the input of the DCX to cover the HET demand. This voltage will be determined by the IV curve of the SA and the SAR control loop.

Finally, as aforementioned the SA voltage will vary around the MPP point. These oscillations will be translated into the HET voltage by the DCX, so they will be scaled by the DCX turn-ratio. This issue is addressed in [18].

2) Separated LV SA

a) Architecture description:

In this architecture there are sections devoted to power solely the bus, (labelled LV BUS SA in Figure 9) and others that can power the HET, through a DCX or the bus (labelled LV HET SA in Figure 9). The interface between the bus and the SAs will be made with independent DCDC converters with MPPT capabilities. Several options appear to control these independent converters. One approach will be to control them by the same MEA voltage. A similar approach has been used in Bepi Colombo MTM [19], [20], where different converters controlled by the same voltage interface with different SA sections.

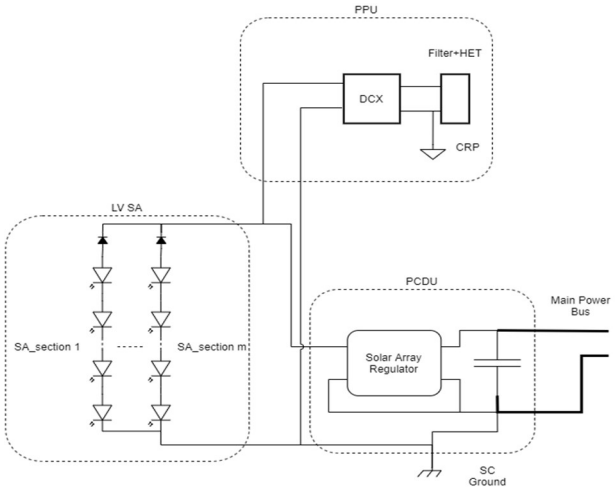

Figure 7: Single SA Low Voltage

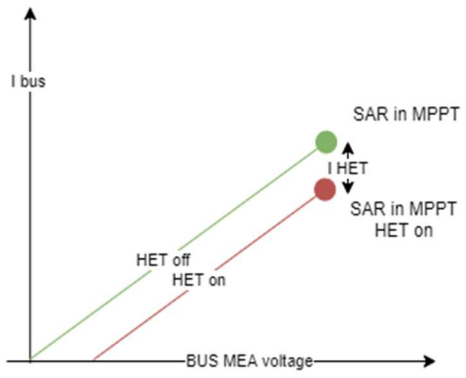

Figure 8: MEA voltage and bus current

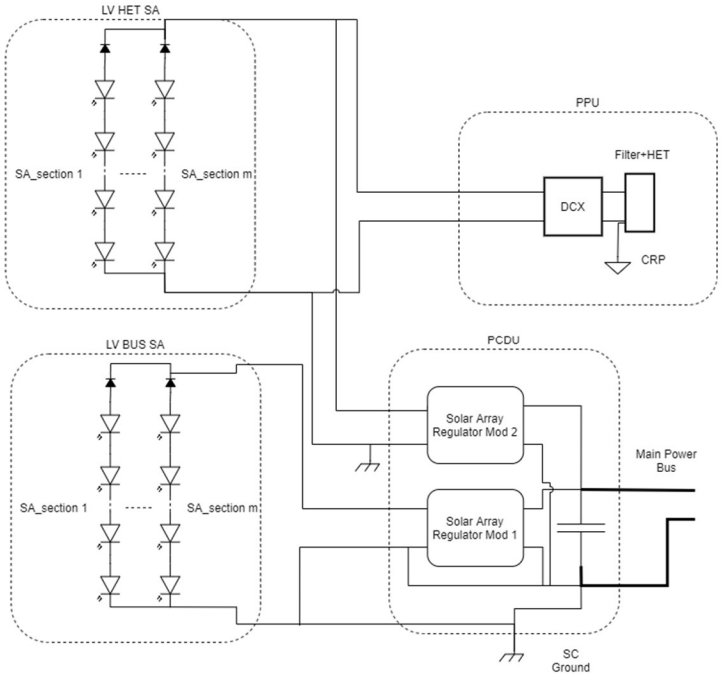

Figure 9: Separated SA Low Voltage

This is what it is represented in Figure 11. In Figure 11a it is represented what happens when the HET is off. The MEA will ask the different modules to provide current. If the bus demand is low only the first module will be providing power. When this first one reaches its MPP it will lock there and the other will supply the rest of the power to cover the bus demand until it reaches its MPP.

When the HET is on, the demand of the HET will be subtracted to its input, then its SAR will get less current and then it will lock into is MPP with a lower bus current. If more current is needed in the bus the other will supply it. This is what it is represented in Figure 11b.

The main advantage over the Single SA architecture is the following. As one of the SA sections (LV HET SA in Figure 9) MPP is matched to the HET demand, once the HET turns on, the SA section is unable to provide the power demand to the bus. Then the SAR module connected to it (Solar Array Regulator Mod 2 in Figure 9) will lock into its V_{mp}. Then, the HET voltage will be regulated by the MPP loop to a voltage $V_{HET} = n_{DCX} \cdot V_{mp}$

This option offers another degree of freedom. If voltage over the HET needs to be precisely regulated during its operation the input voltage of converter Solar Array Regulator Mod 2 could be regulated via an additional dedicated control loop, pretty much as the MPP Tracking method controls the input voltage. This additional input voltage loop will override the output voltage loop for Solar Array Regulator Mod 2. This will diminish the power injected by Solar Array Regulator Mod 2 to the bus. Then, Solar Array Regulator Mod 1 will control the bus voltage injecting the current needed to keep the output voltage regulated. This could be achieved if Solar Array Regulator Mod 2 is not locked into the MPP of the corresponding SA section. The HET will see a scaled version of this regulated input voltage.

Again, as in the Single SA architecture, if SAR Mod 2 is in MPPT mode the SA voltage will oscillate around the MPP point. Also, the DCX will allow to isolate the HET in case of failure.

3) Single SA High Voltage

Based on the single SA architecture the Single SA High Voltage is derived. The idea is to size the SA so its voltage

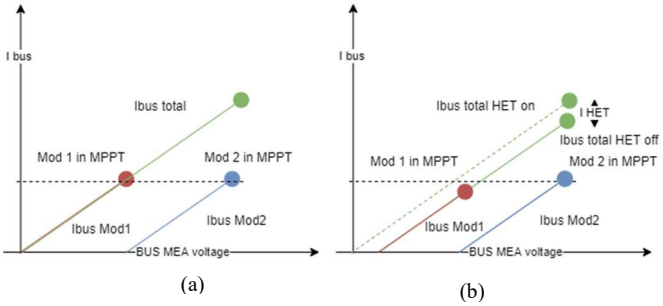

Figure 11: MEA voltage and bus current a) HET off b) HET on

matches the HET voltage as in the Pure DD architecture. Its schematic is shown in Figure 10.

The voltage on the SA is the scaled down by a DCX which then feeds a typical SAR designed to work at a lower voltage. The main problem with this architecture is that the bus is supplied through the DCX and the PCDU, so it is converted twice with the associated losses. In any case it could be interesting for missions in which the bus requires very low power and the EP a very big one. This is similar to what is done in the mission PSYCHE [21], the architecture used to power the low voltage loads in Bepi-Colombo [19] and what it is proposed in the EDDA architecture [14].

In this case the return of the SA is referenced to the CRP, the DCX will perform the isolation for the rest of the SC. If this represent an issue a CRP supply must be added to the architecture, as in Figure 10, with the losses associated.

In this architecture protections regarding the connection of the SA to the HET are needed to avoid potential problems.

4) Separated SA High Voltage

Using the same concept as is single SA High voltage the separated SA architecture is evaluated. In this occasion, as seen in Figure 12, there will be two different SA sections with different voltages. The one devoted to power the HET will be a high voltage one while the other powering the bus will be a low voltage one. The SAR will have two inputs sharing the MEA. The input connected to the high voltage SA section will be connected to the SAR through a DCX so the HV SA is seen by the SAR as a low voltage one.

As in the Single SA HV power to the bus is could be converted twice. However, in this case only the power coming from the HV SA section instead of the full power will be converted twice. In this regard it would be advisable to connect the HV SA section to the converter in the high range of the MEA. In this case, only the excess of demand from what the LV SA section can provide will be converted twice.

In this architecture protections regarding the connection of the SA to the HET are needed to avoid problems.

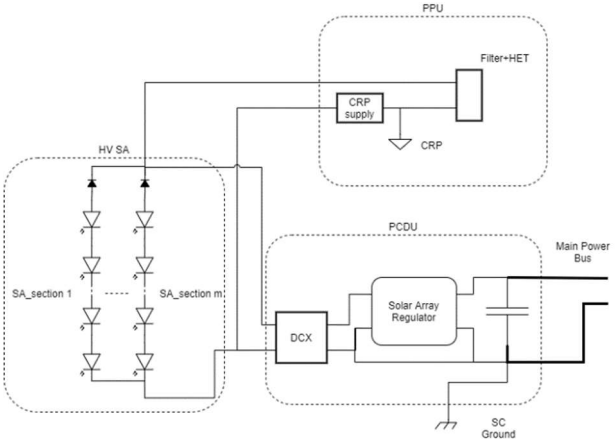

Figure 10: Single SA High Voltage with CRP supply

Electrically wise this solution is analogous to the Separated SA LV

5) Single SA HV system

If the power systems of an SC demand more power, it would make sense to go to higher voltage SA and even buses. However, for calculation purposes it would be assumed that the bus voltage is still 100 V Apart from the HV SA developments regarding high voltage power electronics for interfacing the HV shall be developed. A CRP supply is needed to keep the discharge between anode and cathode.

6) Separated SA HV system

The HV adaptation of the separated LV system is the same as the Separated SA HV without the DCX. The high voltage power electronics are needed for the SAR connected to it. Again, a CRP supply is needed and protections for the HET shall be included.

E. Traditional derived Architectures

In the traditional architecture the power for the discharge supply comes from the power bus. This has the advantage of having a very well-regulated voltage to supply it.

1) Traditional Architecture

The traditional architecture is added to the comparison. It will serve as a reference to see how the proposed architectures behave against it. A MPPT based topology was selected but the results would be very similar using a S3R based one.

2) DCX discharge supply

This architecture derives from the classical one. The difference is that instead of having a typical discharge supply this one has been replaced by a DCX that scales the bus voltage to the HET needs. The benefit is that the DCX presents a higher efficiency than the typical discharge supply. The DCX will provide isolation guaranteeing the discharge between anode and cathode. In some way reminds of the Intermediate Bus Architecture [22]. No regulation is performed inside the PPU towards the HET voltage. It relies on the fact that the bus voltage, especially in the regulated bus architecture, is tightly controlled and presents a very small impedance. Hence it is a very good voltage source that should cope with the discharge current transits, specially at ignition. The filter unit design gets special relevance since it will have to mitigate these transients and the oscillations in the discharge current since in this configuration, they can affect the power bus.

IV. ARCHITECTURE COMPARISON

A. New developments comparison

The new developments needed for implementing the different architectures are represented in Table 1. As it can be seen most of the architectures make use of the DCX. Strictly

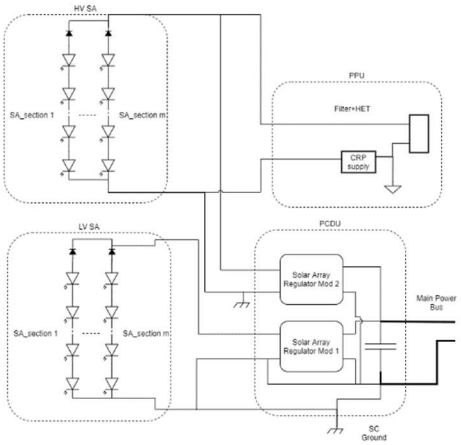

Figure 12: Separated SA High Voltage with CRP supply

speaking these have been presented in [12]. However, they must be adapted for the EP usage.

Several research activities, funded by different ESA and European programs have addressed the development of High Voltge Soalr arrays and High Voltage electronics for space applications. The biggest technological challenges are the ones regarding the SA. Voltages around 300 V are common in power electronics in terrestrial applications. In this regard the 650 V GaN HEMTs from Teledyne [24] are a space ruggedized version of the same part from GaN Systems. These devices could be used for the HV SARs and the DCX. This high voltage devices must be applied to the S3R options. CRP supplies have been developed in the frame of the EDDA project [16] but it will be new for a company building a PPU that needs it. They represent a challenge since it needs to measure both the current in the lines connecting the anode and the cathode of the HET.

Finally, none of the architectures regulate the voltage to the Anode of the HET. Nor they offer a current limit protection. Current control must be performed via the gas flow rate. This would be very interesting specially to find the MPP of the SA in the architectures that devote SAs exclusively to EP, which are most of the proposed ones In these cases, current regulation via gas flow will be interesting to avoid demanding more current than the rated. Regulation via gas flow rate is reported in [5], where it is also coupled to the magnet current control. MPP Tracking methods such as the one reported in [18] could be adapted to it, in this case the control voltage reference will replaced by the reference for the gas flow control loop. This method will introduce oscillations in the discharge voltage as the ones described in [17] but at much lower frequency since the current is varied through a gas flow which is slower than a DC/DC converter. If this gas based MPPT is implemented along a SAR with MPP capabilities precautions must be taken to avoid interaction between the two MPPT

Table 1: New developments

Architecture	New Development	HV SA	HV Electronics	DCX	HV switch	CRP supply	Gas flow discharge current control	MPPT gas flow control
Pure DD		X	X		X	X	X	X
Isolated DD				X			X	X
Semi-Isolated DD				X		X	X	X
Single SA LV				X			X	
Separated SA LV				X			X	X
Single SA HV		X		X		X	X	
Separated SA HV		X		X		X	X	X
Single SA HV system		X	X			X	X	
Separated SA HV system		X	X			X	X	X
Discharge supply DCX				X			X	

Table 2: HET voltage control method

Architecture	Control Method	Current control through Gas Flow rate control	MPPT via converter to Bus	Input voltage and bus voltage
Pure DD		X		
Isolated DD		X		
Semi-Isolated DD		X		
Single SA LV		X	X	
Separated SA LV		X	X	X
Single SA HV		X	X	
Separated SA HV		X	X	X
Single SA HV system		X	X	
Separated SA HV system		X	X	X
Discharge supply DCX				

systems. In Table 1 the MPPT via gas flow is marked in grey to indicate it would be optional.

The current regulation could be improved to discharge power regulation. If the voltage across the HET is sensed, better at the input of the filter unit, and it is multiplied by the discharge current measurement then the gas flow rate could be adjusted to guarantee a desired discharge power, which in turn is related to the thrust. This control could be done digitally. It is important to highlight that in all the architectures, but the Discharge Supply DCX the discharge voltage will be related to the IV curve of the SA. Interaction of the thrust control and the MPPT operation via discharge flow needs also to be studied.

The capability of regulating the voltage to the HET is represented in Table 2. Every architecture, but Discharge supply DCX offers some degree of controllability to the voltage of the HET. In this later case the voltage over the HET will always be a scaled version of the bus voltage. In all the remaining cases the discharge current can be controlled via the gas flow rate. As the HET will always see a version of the IV of the SA its voltage can be controlled this way. However, it will have implications to the ISP and thrust. In all the options which have an MPPT capable converter the input voltage, and hence the HET voltage will eventually lock into the MPP of the SA. This offers a limited way of controllability. With a single SA, once the MPP is locked if the discharge current is varied, via the gas flow rate, the voltage will remain the same providing that the bus can tolerate the power variation, either by charging or discharging the battery or by compensating the change in the HET demand activating or deactivating loads such as heaters or ballast. However, this is a temporary solution since no SC, unless is specially designed to do so, tolerate this mode of operation for extended periods of time.

The most flexible option will be offered by the Separated SA options. Most of SC converters are current programmed ones [25], [26]. This means that the current through a component of the converter, most commonly an inductor, is regulated to a reference value. A voltage control loop sets the reference for the current loop. For bus voltage regulation this loop controls the output voltage of the converter. However, for MPPT control the input voltage or the current set this reference [18]. An input voltage control loop can be implemented to regulate it by setting the current reference. This input voltage loop can override the output voltage one. If this happens the voltage at the HET, which in the separated options is either the SA section voltage or a DCX scaled version of it, will be regulated via this loop between the V_{mp} and the V_{oc} of the SA section. In this architecture one SA section is sized to provide the nominal HET power and nothing to the bus. Hence the other converter in the architecture, which will be controlled by its output voltage, will inject the current needed to keep the bus voltage. This converter is connected to a SA section sized to power the SC demand minus the HET. If the voltage over the HET is regulated above V_{mp}, the power to the HET will be smaller and this converter can inject some power to the bus. Therefore, the second one will inject less. This input voltage loop needs to address the issues described in [22].

B. *Performance comparison*

1) *Spacecraft definition*

Given the variety of SC and missions that can benefit for these architectures a common ground to defined the SC is presented here. All the solutions presented in this work are evaluated following this process:

- The total SC power,$Power_{SC}$, bus voltage and HET voltage are inputs of the design.
- The power of the EP is defined fixing Ep_ratio
$$Ep\_ratio = {Power\_EP}/{Power\_SC} \quad (10)$$
- The power of the payload is defined by fixing Pay_ratio
$$Pay\_ratio = {Power\_pay}/{Power\_SC} \quad (11)$$
- It will be assumed that when the EP is in use the payload is not. Therefore, the platform power is defined as
$$Power\_platform = Power\_SC - Power_{EP} \quad (12)$$
- A solar cell is defined for calculating the SAs are selected.
- Depending on the architecture, starting from the Total SC power or the EP power and platform power, the SAs are calculated. SA calculation considers the efficiency of the conversion stages between SA an EP or bus. No thermal effects have been considered in the SAs. It is assumed that the cells are in the conditions given in the datasheet.
- The mass of the SAs and the power conversion stages is calculated. With this the figures for the comparison described in section IV.B.2) are calculated.

Although simplifications have been made, they are the same for all the different architectures. The exact numbers may have some imprecisions but there will be the same for each architecture. For example, the SAs may be bigger for

addressing the thermal behaviour, but they should be bigger in all the architectures. Therefore, the comparison is fair.

Finally, two more figures can be used to determine how often the EP is in use. These are:

- Duty mode: When the EP mode is in use the percentage of time the propulsion is on and hence there is a great power consumption.
- Duty mission: Through the whole mission the percentage of time the EP mode is on.

At the end the percentage of time the EP is on during the mission would be the product of both Duty mode and Duty mission.

The aforementioned figures serve to define the different use cases. Different missions will have different figures. While there may be many different missions some of the most typical that can be identified from the literature are these 4 use cases: A GEO telecommunications satellite with electric orbit raising and station keeping (GEO-T). An Earth observation satellite in a very low orbit so drag needs to be constantly compensated (LEO-D). A Cruise in which a spacecraft goes to deep space using electrical propulsion and then performs its mission, and then finally a Tug in which a spacecraft provides another (or several others) with transportation. An example is shown in Table 3 where GEO-T is a telecom satellite from MAXAR [23], LEO-D is modelled after GOCE [24], the Cruise is modelled after PSYCHE [25], [26] and the Tug after Bepi-Colombo MTM[19], [27]. It can be seen how, with the exception, of the Tug and LEO-D the usage of EP during a mission is rather low. This builds a strong case for the reutilization of the installed power either for the load or the platform. The best solution would depend on the specifics of each mission.

Table 3: EP use cases

	GEO-T	LEO-D	Cruise	Tug
Duty_mode	94%	100%	13%	100%
Duty_mission	4%	91%	8.3%	47%
EP_ratio	66.7%	48%	45%	71%
Payload_ratio	55.5%	7.7%	32%	11%

2) Comparison figures

All the options presented in this work are compared against the same figures. These figures try to reflect the performance of each solution.

- Installed Power (W): How much power an SA must produce to satisfy the power demands of the SC. It considers the efficiency of each power conversion stage.
- Bus Power (W): How much power is needed in the power bus. Bear in mind that the Discharge power in DD systems usually does not comes from the power bus. It also considers how much of the power used by the discharge can be utilized by the bus when EP is not in use, considered the inefficiencies between the power source of the discharge and the bus.
- Bus utilization (%): Bus utilization is the ratio between Bus Power and Installed Power

$$bus_{util} = {power_{bus}}/{power_{installed}} \quad (13)$$

It is an adimensional figure which reflects how well a power architecture can deliver power to the bus when the EP is not in use.

- Total SA mass (Kg): Starting from the Installed power a model for the mass of the SA is used to calculate how much mass in SA is needed. These considers the mass of the solar cells and a model of the mechanical structure supporting the panel. Section III.A shows the assumptions made for these calculations. The SA is the main contributor of the total mass.
- Total mass (Kg): Based on the number and power rating of the different power conversion units needed, namely SARs, S3Rs, DCXs, CRP supplies and isolation switches, the mass of the power system is estimated and added to the total SA mass.
- Bus power mass ratio (W/Kg): This is the ratio of the Bus power divided by the total mass.

$$bus_{pow\ \ mass} = {power_{bus}}/{mass_{total}} \quad (14)$$

- Total power mass ratio (W/Kg): This is the ratio of the Total installed power divided by the total mass.

$$power_{mass} = {power_{total}}/{mass_{total}} \quad (15)$$

- Efficiency supplying the HET (%): As the main goal of Direct Drive architectures are to increase the efficiency on the power delivery to the discharge supply of the HET this figure addresses it

$$\eta_{HET} = \frac{P_{HET}}{P_{HET}+losses_{HET}} = \frac{P_{HET}}{P_{HET\_in}} \quad (16)$$

One important point appears on how to model the efficiency of an architecture using the CRP supply. If a DCX or a power converter supplies the HET, the term $losses_{HET}$ models the dissipation in DCX or power converter supplying the HET. However, as seen in Figure 13 the full current discharge circulates through the CRP supply while it will keep a voltage $v_{crp-ground}$ between the CRP and the ground. This voltage will be controlled so the current going into the anode is the same as the current retuning through the cathode. This voltage varies depending on the environmental conditions [3]. In this reference it is shown that for having a discharge current returning from the structure of 0 A -18 V are needed, for this work it will be assumed that $v_{crp-gnd} = -15\,V$. It will be assumed that its power will come from the power bus, as the rest of the power supplies in the PPU (magnet, flow control, etc.). A simplified schematic is represented in Figure 13. The total voltage over the SA will be determined by the discharge current $I_{discharg}$, or it will be fixed to its maximum power point V_{mp} as described in section III.D . Then, the voltage over the HET will be $V_{HET} = V_{SA} - V_{crp-g}$. For simplification purposes it will be assumed that V_{HET} and $I_{discharge}$ are the nominal ones that configure the power demand of the HET.

$$P_{HET} = V_{HET} \cdot I_{discharge} \quad (17)$$

The power supplied by the CRP supply will be

$$P_{CRP\_out} = \left|V_{crp-gnd} \cdot I_{discharge}\right| \quad (18)$$

To supply this power the CRP supply will demand

$$P_{CRP\_in} = \frac{P_{CRP_{out}}}{\eta_{CRP}} = V_{bus} \cdot I_{CRP_{in}} \quad (19)$$

Then the efficiency in supplying the HET whilst having a CRP supply will be calculated as

$$\eta_{HET} = \frac{P_{HET}}{P_{HET}-P_{CRP\_out}+P_{CRP\_in}} \quad (20)$$

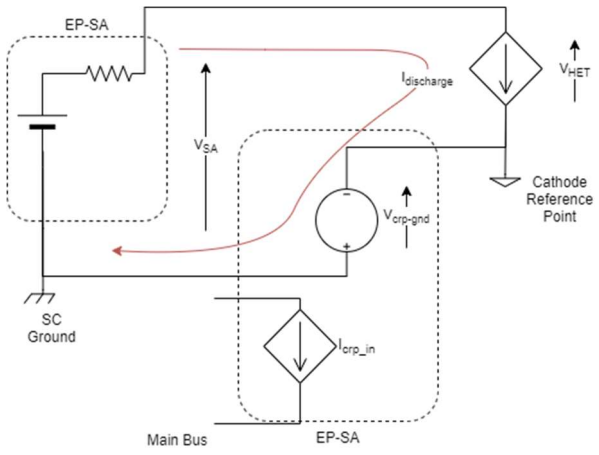

Figure 13: CRP power simplification

Then the SA should be sized so its voltage at operation, being the one fixed by the discharge or V_{mp}, plus the maximum expected $v_{crp-gnd}$. If this in not carried out the voltage of the SA can be lowered by the action of the CRP supply and make the SA behave as a current source. Due to the current supply behaviour of the discharge this can cause problems, as two current sources will be placed in series. This situation shall be monitored and corrected via diminishing the gas flow rate and thus reducing HET current and power.

Other possibility will be assuming that the voltage over the HET is $v_{crp-gnd}$ volts below its nominal voltage. Because of the current source behaviour of the discharge current will make its power being:

$$P_{HET\_crp} = \left(V_{HET} - v_{crp-gnd}\right).I_{discharge} = P_{HET} + P_{CRP\_out} \quad (21)$$

Then the efficiency shall be calculating replacing P_{HET} by P_{HET_crp}

$$\eta_{HET} = \frac{P_{HET}+P_{CRP\_out}}{P_{HET}+P_{CRP\_in}} \quad (22)$$

In any case the first approach has been followed since it conserves the power to the HET and therefore the comparison with the systems that do not use a CRP supply is fairer. It will be assumed that this voltage is negative as it seems to be the case. However, [3] cites the SMART-1 results in which this voltage is positive. If this is the case the associated converter will absorb power, either dissipating it or transferring it to the bus. In the experiments carried out in [3] it is explicitly mentioned that a voltage source capable of absorbing power is used. In either case this will mean a complicated design and control for the CRP supply.

- To model the total efficiency in supplying the HET the following figure will be calculated:

$$\eta_{HET\_total} = \frac{P_{HET}+P_{CRP\_out}}{P_{HET\_in}+{P_{CRP\_in}}/{\eta_{bus}}} \quad (23)$$

Where P_{HET} is the nominal HET power, P_{HET_in} is the power consumed in the stages supplying the HET from the SA, P_{CRP_out} is the power that is supplied by the CRP supply, P_{CRP_in} is the power demanded by the CRP supply to perform its function. Finally, η_{bus}, is the efficiency of the power system, then ${P_{CRP\_in}}/{\eta_{bus}}$ models the power demanded to the SA to supply the CRP voltage.

- Efficiency of the Installation (%): Is adimensional, it is the ratio of the total power required by the SC and the total power installed. It measures how well the SC utilizes the installed power.

$$eff_{install} = {power\_total}/{power\_installed} \quad (24)$$

Finally, the following figures try to shine a light on the size of the needed radiators. Three dissipation figures are calculated.

- Dissipation PCDU Payload (W): This indicates how much power is dissipated in the conversion stages inside the PCDU to supply the payload. In some cases, such as Telecom satellites the payload is almost of the same power as the EP and it is use for much more time. Therefore, it will be a main driver on the thermal design. In other cases, the payload power is much less relevant.
- Dissipation PCDU EP (W): This models the dissipation of the PCDU when the EP is in use. To have a fair comparison the PPU consumption regarding heaters, magnets, control etc is not evaluated, since it will be equal for all. In most of the presented architectures it models the dissipation associated to the CRP supply demand. In traditional architecture it models the losses in the PCDU that occur when supplying the discharge.
- Dissipation PPU (W): This models the total dissipation on the PPU when EP is in use, mainly DCX and CRP supplies if used.

3) Tool Description

A tool to analyse the different options have been developed. This tool is developed in Python. It consists of a series of Jupyter notebooks, so the user can interface easily with them and a series of Python libraries that are used to make the calculations. Finally, all the architectures are calculated for a given use case. A comparison of the architectures for such a case is presented to the user.

C. Architecture comparison example

As an example of the usage of the tool is shown in for the following input data:

- Bus voltage: 100 V
- HET Voltage: 300 V
- SC Power: 14 kW
- $EP\_ratio = {Power\_EP}/{Power\_SC} = 0.5$
- $Pay\_ratio = {Power\_pay}/{Power\_SC} = 0.05$

With this input data all the architectures are generated, and the figures described in section IV.B.2) calculated. These figures are used to evaluate what would be the better solution for the afore described SC.

The install efficiency measures how well the SC utilizes the installed power. It will benefit the solutions that provide a installed power closer to the SC power. Results are seen in Figure 14. It can be seen how a lot of the solutions reach values above 90% but the pure DD is around 70%. Interestingly the traditional solution, PPU_MPPT, is close to 81%. Pure DD is penalized because when the EP is not in use the MPP of the HV SA is very far from the bus voltage.

The objective of the study is summarized in Figure 18. There it is represented the total power efficiency in supplying the HET and the install efficiency, how much overhead in installed power do I need to supply the total SC power. The best solution is the one closest to upper left corner. In this case is the single SA HV system.

One of the reasons behind DD architectures is the improvement of the power efficiency supplying the HET. This is represented in Figure 15. All the proposed solutions reach an efficiency much higher than 90%. However, one of the most interesting solutions would be PPU_DCX_MPPT, this is just replacing the discharge supply of a typical PPU by a DCX, so the voltage of the HET is just a scaled version of the bus. In this case the development effort would be very minor.

Figure 17 represents the dissipation in the PCDU when the EP is in use. And in Figure 16 the same figure when the payload is in use. It can be seen how the in the approaches in which the power of the EP pass through the PCDU have the biggest dissipations, being the EP the sizing case for the PCDU radiators.

Another interesting figure is to plot for a fixed SC power what solution would be the best for increasing EP ratios. That is, more power devoted to electrical propulsion. The previously explained analysis have been redone for different EP ratios. The results can be seen in Figure 19 shows the same plot only for the architectures presented in this paper. where the Efficiency on supplying the HET (vertical axis) is represented against the Installation Efficiency (horizontal axis). Each of the individual axis represent a different EP ratio between 10% to 95%. Best architectures would be situated on the rightmost corner of each of the axes. In every situation the best solution would be either to have a high voltage system with high voltage solar arrays SAR and bus (singleSA_HV_sys) or with the same HV bus two separate Sas (sepSA_HV_sys). The second best would depend on the EP ratio. At low EP ratio it seems to have a separate HV SA to power the EP and then scale it to power the bus through a DCX (sep_SA_HV). However, as the EP ratio increases the second-best solution would be to have a single HV SA (singleSA_HV) with a low voltage bus, then using high voltage power conversion stages. Traditional PPU design is always the worst in both terms. The solutions using low voltage SA rank slightly worst in terms of HET efficiency but almost on par on install efficiency. Pure DD always is penalized in terms of Install efficiency due to the voltage mismatch. As the EP ratio grows there is more power to supply to the low voltage bus when the EP is not in use and thus this is why as EP ratio increases its install efficiency decreases.

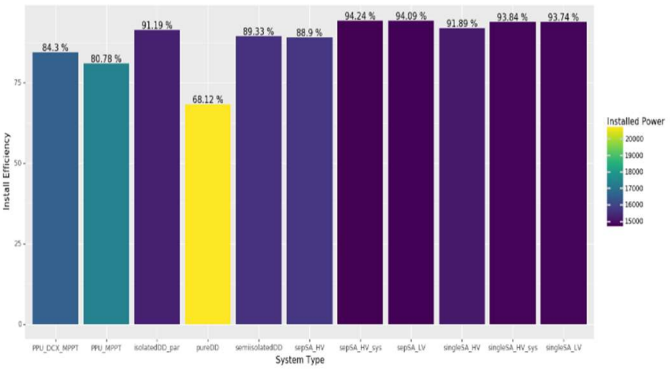

Figure 14:Installation efficiency

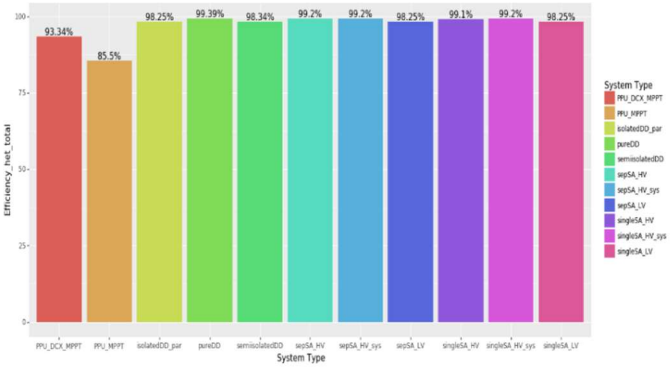

Figure 15:Total efficiency supplying the HET

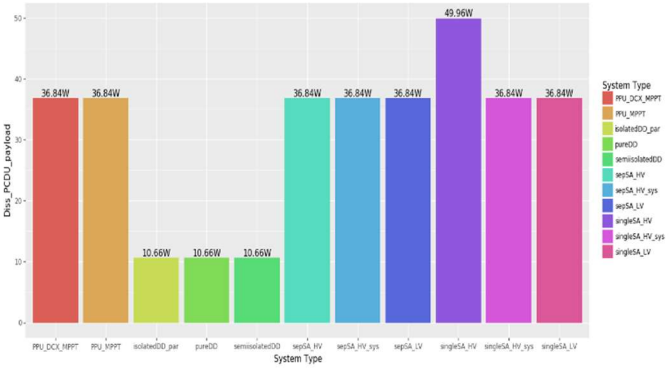

Figure 16: Dissipation in PCDU when payload is in use

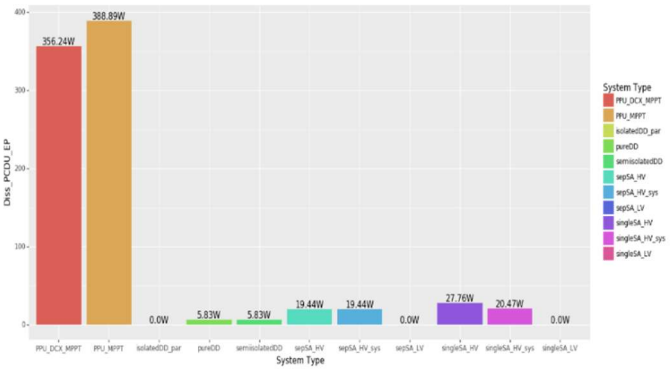

Figure 17: Dissipation in PCDU when EP in use

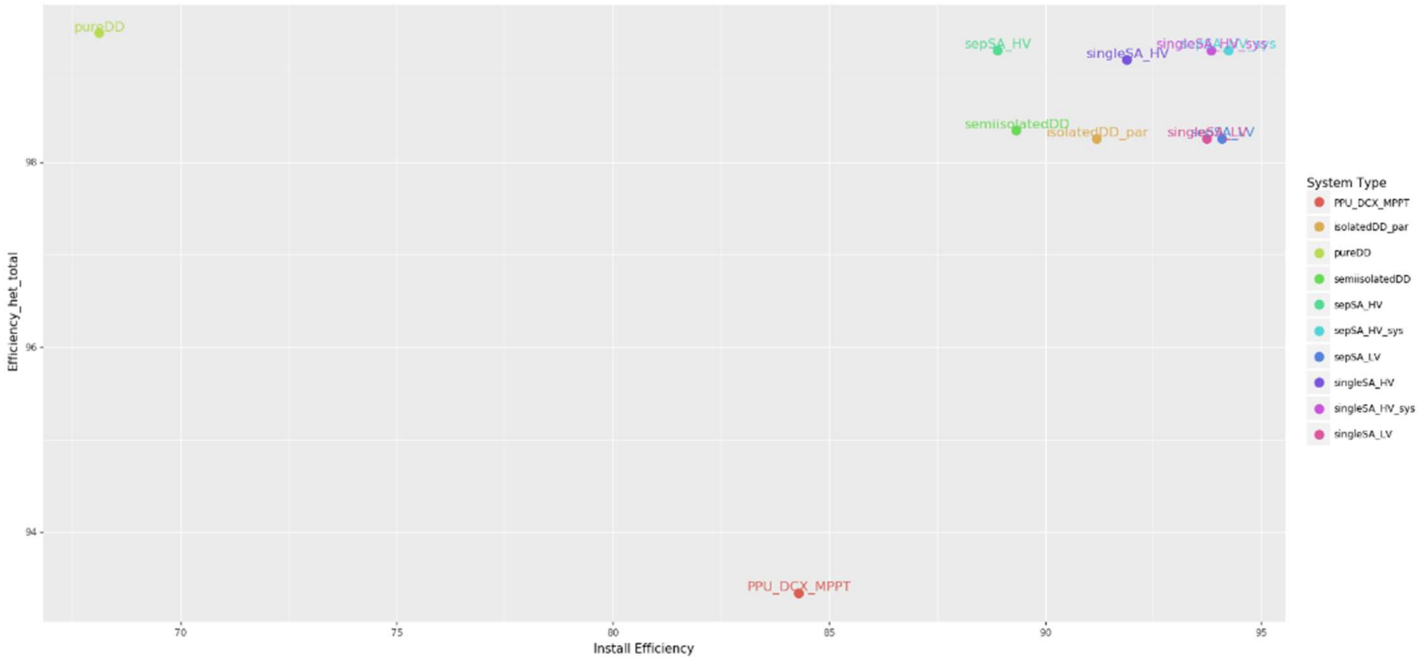

Figure 18: Power efficiency supplying the HET vs. Installation Efficiency

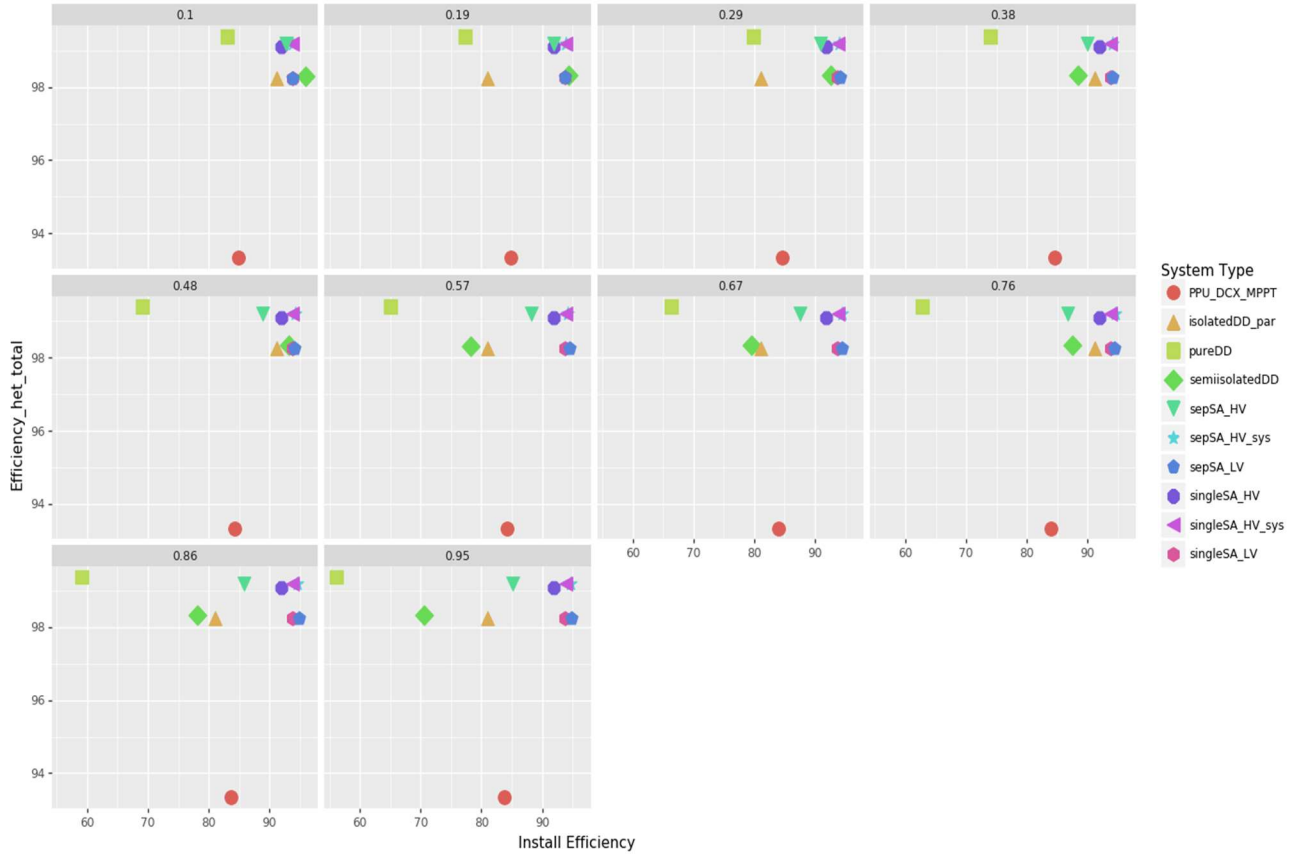

Figure 19: Efficiency HET vs Installed Efficiency for the proposed architecures

V. CONCLUSIONS

In the architectures based on the S3R pairing high voltage SA with lower voltage buses will result in installed power that cannot be utilized for any other purpose than the EP. This can be seen in the analysis with the Pure DD architecture. Especially regarding the Install Efficiency metric. If the power bus is distributed at 300 V the results will be much different, but then the secondary power system will have to scale the voltage from the bus to the loads.

Better results appear when High Voltage SA are combined with converter-based power system. This allows to scale the HV SA to a 100 V bus, keeping the rest of the power system untouched. However, converters and specially, semiconductor devices needed to deal with these voltages are needed.

Scaling up the voltage of SAs with high efficiency DCX results in flexibility to use power systems with different EP and bus voltages This is especially relevant in the S3R cases. Moreover, while introducing a small penalty in the form of losses, DCXs avoid the use of High Voltage Solar Arrays which are still in development. On the other hand, DCX use techniques, material devices and processes common to the Power Electronics domain so its development would be much easier. As explained the inputs of the DCX can be connected in series, thus reducing the voltage that its constituent switches must withstand. This opens the door to use common space grade devices rated at 100 V.

A direct connection between the SA and the thruster will imply double insulation between the SA and the thruster and the inclusion of protection devices, which will affect the power efficiency and have not been considered in the study. The inclusion of power conversion stages such as the DCX between the SAs and the thruster alleviates this because the DCX can double as a protection device. Specially, if it is based in a full-bridge structure since this structure is reliable against a short-circuit in one of the transistors. In this case it would be enough to command open all the transistors to isolate the DCX from its power source (SA or bus).

None of the presented architecture allows for a precise control of the anode voltage. In most cases its voltage will depend on the discharge current following the IV curve of a Solar Array. The PPU-DCX architecture will provide a fixed scaling of the bus voltage, although a set of reconfigurable DCX with different turn-ratio options or with its outputs in series could be envisioned if different voltage ranges are needed for different thruster operation points. Only a limited range of controllability, between the V_{mp} and the V_{oc} of the SA used to power the EP could be introduced in the SEP_SA architectures by controlling the input voltage of the said SA. However, this requires further investigation regarding the interaction with the rest of the power system.

The lack of controllability of the anode voltage has an impact on EP management. Thrust is related to the discharge current. Specific Impulse (ISP) is related to anode voltage. As in most cases they are coupled through the IV curve of a SA. These IV curve will vary with the solar irradiation, the temperature, the degradation, and the impact over the propulsion performance needs to be assessed.

Regarding MPP methods. Due to the lack of regulation the oscillations that the most common used methods impose over the SA will be translated to anode of the HET. These oscillations will have an impact, at least, to the thrust and the ISP which needs to be assessed by EP experts. The effect of such oscillations could be minored through proper design of the Filter Unit, which will lead to bigger reactive components. Then a system level decision needs to be made.

Results of the PPU-DCX architecture shows that by addressing the efficiency issue of the discharge supply good results can be achieved through a traditional architecture with two conversions in cascade. If the typical efficiency of the discharge supply could be raised to 98% the results between traditional PPU designs and PPU-DCX designs will be getting the same performance regarding installed efficiency and power efficiency whilst keeping full controllability of the anode voltage, leveraging the tight regulation of the bus voltage.

ACKNOWLEDGEMENTS

This work has been carried out under ESA funding through project STUDY ON DIRECT DRIVE TOPOLOGIES FOR ELECTRICAL PROPULSION as per Statement of Work (SoW) ref. 1300057583 and through the project PID2021-127707OB-C21 from the Spanish Ministry of Science and Innovation.

BIBLIOGRAPHY

[1] J.-P. Boeuf, 'Tutorial: Physics and modeling of Hall thrusters', *J. Appl. Phys.*, vol. 121, no. 1, p. 011101, Jan. 2017, doi: 10.1063/1.4972269.

[2] D. M. Goebel and I. Katz, *Fundamentals of electric propulsion: ion and Hall thrusters*. in JPL space science and technology series, no. 1. Hoboken, N.J: Wiley, 2008.

[3] L. Ghislanzoni, L. Benetti, T. Misuri, G. Cesaretti, and L. Fontani, 'Hall Effect Thruster Direct Drive PPUs, Experimental Investigation of the Cathode Potential Grounding Problem', *E3S Web Conf.*, vol. 16, p. 15002, 2017, doi: 10.1051/e3sconf/20171615002.

[4] J. A. Hamley, 'Direct drive options for electric propulsion systems', *IEEE Aerosp. Electron. Syst. Mag.*, vol. 11, no. 2, pp. 20–24, Feb. 1996, doi: 10.1109/62.484301.

[5] John Steven Snyder, John R.Brophy, Richard R. Hofer, Dan M. Goebel, § and Ira Katz, 'Experimental Investigation of a Direct-Drive Hall Thruster and Solar Array System at Power Levels up to 10 kW',

[6] T. A. Schneider *et al.*, 'Solar Arrays for Direct-Drive Electric Propulsion: Arcing at High Voltages', *J. Spacecr. Rockets*, vol. 42, no. 3, pp. 543–549, 2005, doi: 10.2514/1.5636.

[7] I. G. Mikellides, G. A. Jongeward, T. Schneider, T. Peterson, T. W. Kerslake, and D. Snyder, 'Solar Arrays for Direct-Drive Electric Propulsion: Electron Collection at High Voltages', *J. Spacecr. Rockets*, vol. 42, no. 3, pp. 550–558, 2005, doi: 10.2514/1.5609.

[8] 'Space Engineering-Electrical and electronic'. ECSS Secretariat ESA-ESTEC Requirements & Standards Division Noordwijk, The Netherlands, Oct. 15, 2019.

[9] 'SA50-120 Single Series datasheet'. Microsemi.

[10] S. Kimmelmann and W. Knorr, 'High Efficient Universal Buck Boost Solar Array Regulator SAR Module', vol. 719, p. 38, Aug. 2014.

[11] E. Lapeña, J. L. Herranz, F. Gómez-Carpintero, and M. Rodríguez, 'The LEO PCDU EVO - A Modular and Flexible Concept for Low to Medium Power LEO & Scientific Missions', *E3S Web Conf.*, vol. 16, p. 18009, 2017, doi: 10.1051/e3sconf/20171618009.

[12] Manuel Arias Perez de Azpeitia, 'Final report for the activity Regulated Power System Building Block Study ESA-TEC-SOW-008509'.

[13] '3G30A Triple Junction Cell datasheet'. AzurSpace.

[14] Jean-Baptiste De Boissieu, 'Direct-Drive Architecture for Solar Electric Propulsion', presented at the Conference on Advanced Power Systems for Deep Space Exploration, VIRTUAL EVENT, Oct. 2020.

[15] J. M. Blanes *et al.*, 'Two-Stage MPPT Power Regulator for Satellite Electrical Propulsion System', *IEEE Trans. Aerosp. Electron. Syst.*, vol. 47, no. 3, pp. 1617–1630, Jul. 2011, doi: 10.1109/TAES.2011.5937254.

[16] A. K. Podder, N. K. Roy, and H. R. Pota, 'MPPT methods for solar PV systems: a critical review based on tracking nature', *IET Renew. Power Gener.*, vol. 13, no. 10, pp. 1615–1632, 2019, doi: 10.1049/iet-rpg.2018.5946.

[17] A. Fernandez, C. Baur, and F. Gomez-Carpintero, 'Solar Array Hysteresis and its Interaction with the MPPT System', presented at the European Space Power Conference, Noordwijk, Netherlands, 2014.

[18] Pablo F. Miaja *et al.*, 'Co-simulation of Electrical propulsion and power systems in Direct Drive applications', presented at the European Space Power Conference, Elche, Spain, Oct. 2023.

[19] M. Pierluigi, G. Giuseppe, and C. Giuseppe, 'BEPICOLOMBO ELECTRICAL POWER SYSTEM', presented at the European Space Power Conference, Jun. 2011, p. 8.

[20] E. Lapeña *et al.*, 'Boost-based MPPT for the MTM PCDU of the Bepicolombo mission', in *Proceedings of the 8th European Space*

Power Conference (CD-Rom) | 8th European Space Power Conference (ESPC) | 14/09/2008-18/09/2008 | Konstanz, Alemania, Noordwijk, Netherlands: E.T.S.I. Industriales (UPM), 2008, pp. 0–0. Accessed: Oct. 31, 2021. [Online]. Available: http://www.congrex.nl/08a02/

[21] ShaneMalone *et al.*, 'Deep Space Power Processing Unit for the Psyche Mission', in *Deep Space Power Processing Unitforthe Psyche Mission*, Vienna, Sep. 2019.

[22] D. F. D. Tan, 'Intermediate bus architectures: A practical review', in *2013 25th International Symposium on Power Semiconductor Devices IC's (ISPSD)*, May 2013, pp. 19–22. doi: 10.1109/ISPSD.2013.6694471.

[23] I. Johnson *et al.*, 'Maxar's All-EP Spacecraft', in *AIAA Propulsion and Energy 2020 Forum*, in AIAA Propulsion and Energy Forum. American Institute of Aeronautics and Astronautics, 2020. doi: 10.2514/6.2020-3606.

[24] 'GOCE System System Critical Design Review'. May 2015.

[25] W. Hart *et al.*, 'Overview of the spacecraft design for the Psyche mission concept', in *2018 IEEE Aerospace Conference*, Mar. 2018, pp. 1–20. doi: 10.1109/AERO.2018.8396444.

[26] John Steven Snyder, Dan M. Goebel, Vernon Chaplin, Alejandro Lopez Ortega, Ioannis G. Mikellides, Faraz Aghazadeh, Ian Johnson, Taylor Kerl, Giovanni Lenguito, 'Electric Propulsion for the Psyche Mission', presented at the International Electric Propulsion Conference, Vienna, Sep. 2019.

[27] C. Steiger, E. Montagnon, F. Budnik, S. Manganelli, A. Altay, F. Striedter, H. L. Gray, J. Bolter, N. Wallace, O. Sutherland, 'BepiColombo – Solar Electric Propulsion System Operations for the Transit to Mercury', presented at the International Electric Propulsion Conference, Vienna, Sep. 2019.